Device Physics of Solution-Processed Organic Field-Effect Transistors**

By *Henning Sirringhaus**

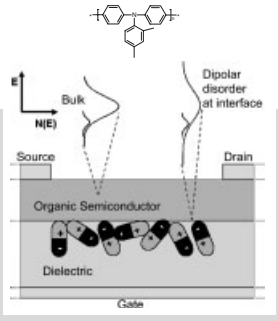

Field-effect transistors based on solution-processible organic semiconductors have experienced impressive improvements in both performance and reliability in recent years, and printing-based manufacturing processes for integrated transistor circuits are being developed to realize low-cost, large-area electronic products on flexible substrates. This article reviews the materials, charge-transport, and device physics of solution-processed organic field-effect transistors, focusing in particular on the physics of the active semiconductor/dielectric interface. Issues such as the relationship between microstructure and charge transport, the critical role of the gate dielectric, the influence of polaronic relaxation and disorder effects on charge transport, charge-injection mechanisms, and the current understanding of mechanisms for charge trapping are reviewed. Many interesting questions on how the molecular and electronic structures and the presence of defects at organic/organic heterointerfaces influence the device performance and stability remain to be explored.

1. Introduction

Following the initial demonstration of field-effect conduction in small organic molecules[1,2] and conjugated polymers,[3–5] the community of industrial and academic research groups that are interested in using organic semiconductors as the active layer in organic field-effect transistor (OFET) devices has been growing steadily, particularly over the last four to five years. The Institute for Scientific Information (ISI) Web of Science counts 393 scientific publications in the field of organic transistors in 2004, up from 304 in 2003, and 80 in 1999. The reasons for this surge of interest are manifold. The performance of OFETs, which is generally benchmarked against that of amorphous silicon (a-Si) thin-film transistors (TFTs) with field-effect mobilities of 0.5–1 $cm^2 V^{-1} s^{-1}$ and ON/OFF current ratios of 10^6–10^8, has improved significantly. Currently, the record mobility (μ) values for thin-film OFETs are 5 $cm^2 V^{-1} s^{-1}$ in the case of vaccum-deposited small molecules[6] and 0.6 $cm^2 V^{-1} s^{-1}$ for solution-processed polymers.[7] As a result, there is now a serious level of industrial interest in using OFETs for applications that are currently incompatible with the use of a-Si or other inorganic transistor technologies. OFETs are most commonly manufactured using standard top-gate (Fig. 1A) and bottom-gate TFT architectures. One of their main technological attractions is that all the layers of an OFET can be deposited and patterned at low/room temperature by a combination of low-cost solution-processing and direct-write printing, which makes them ideally suited for realization of low-cost, large-area electronic functions on flexible substrates (see the reviews by Sirringhaus et al.[8] and Forrest[9]). The first applications in which we can realistically expect OFETs to be used within the next three to five years are flexible, active-matrix electronic-paper displays, for which impressive demonstrations have been developed recently,[10,11] and simple, low-cost, radiofrequency identification (RFID) tags[12] and sensing devices. Other applications, such as active-matrix liquid crystal or organic light-emitting diode (OLED) displays, or high-performance RFID tags compatible with existing communication standards, are also being envisioned,

[*] Prof. H. Sirringhaus
Cavendish Laboratory, University of Cambridge
Cambridge CB3 OHE (UK)
E-mail: hs220@phy.cam.ac.uk
Prof. H. Sirringhaus
Plastic Logic Ltd.
34/35 Cambridge Science Park
Cambridge CB4 OFX (UK)

[**] It is a pleasure to acknowledge stimulating discussions on scientific issues discussed in this review with many wonderful students, postdocs, and colleagues, in particular, Dr. Lukas Buergi, Jana Zaumseil, Shalom Goffri, Tim Richards, Jui-Fen Chang, Dr. Jerome Cornil, Dr. Janos Veres, Dr. Catherine Ramsdale, and Prof. Richard Friend.

DOI: 10.1002/adma.200501152

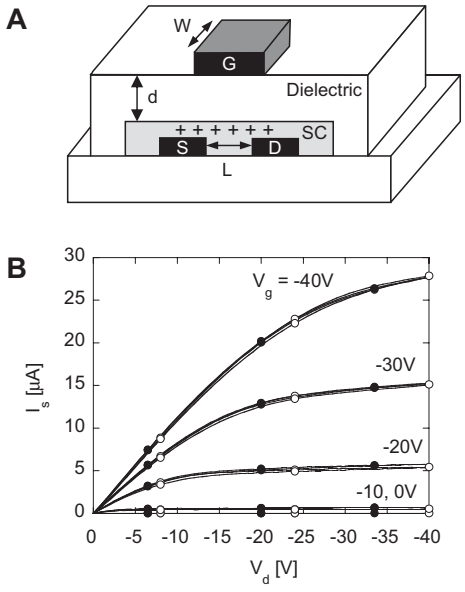

Figure 1. A) Schematic diagram of a top-gate OFET using a standard TFT device architecture. B) Output characteristics (drain voltage, V_d, vs. source current, I_s) of a state-of-the-art, unencapsulated OFET measured in air and light (closed circles: device measured after manufacture; open circles: device measured two weeks later).

but require a transistor performance with mobilities exceeding 1 $cm^2 V^{-1} s^{-1}$, which is still difficult to achieve with solution-processed OFETs.

On the materials front, improving field-effect mobilities remains an important topic, although, compared to the situation in 2002,[13] there has been less emphasis on improving headline mobility numbers and more on developing materials that allow the combination of high mobilities with good materials stability under air, moisture, and light exposure. Very significant progress has been made in this respect recently. Figure 1B shows the output characteristics of a state-of-the-art, unencapsulated polymer FET, comparing measurements performed in ambient air and light directly after device manufacture and several weeks later, after the device had participated in a customer trial and had crossed the Atlantic twice.[11] No evidence for device degradation is observed. Improvements in shelf as well as operational life have been achieved as a result of using organic semiconductors with better inherent stability, better understanding of the requirements for gate dielectrics, and by more controlled manufacturing processes. It is generally well appreciated now that the choice of the right dielectric is crucial for achieving optimum field-effect mobility (μ_{FE}), device stability, and reliability. While most of this work has traditionally focused on the p-type conduction regime, there has been a significant effort made to understand the conduction processes involving negative electrons, with the aim of realizing solution-processible n-type as well as ambipolar organic semiconductors for use in complementary metal oxide semiconductor (CMOS)-type circuits and light-emitting FETs.

There is a wealth of fundamental scientific questions regarding the charge-transport and charge-injection physics of organic semiconductors, and their structure–property relationships, for which FET devices provide a useful scientific tool through their ability to control the charge-carrier concentration electrostatically rather than chemically. A significant effort has been focused on understanding the fundamental electronic structure of the organic semiconductor, in particular at the interface with the dielectric, and how microscopic, molecular-scale transport processes determine the electrical characteristics of macroscopic devices. This is a challenging task because of the complex microstructure of solution-processed organic semiconductors, which in many cases cannot be fully characterized by conventional diffraction and microscopy techniques. An important related topic is the understanding of electronic-defect states and associated device degradation mechanisms, which are becoming an increasingly important topic as OFETs are nearing their introduction into first products with strict reliability and lifetime requirements.

This article is focused on reviewing the current state of knowledge of the materials and the device and charge-transport physics of solution-processed OFETs. Due to limitations of space, no attempt is made to review the device physics of polycrystalline, small-molecule organic semiconductors deposited by vacuum evaporation, nor to give an overview of the different approaches to manufacturing OFETs. For these important subjects we refer the reader to other excellent and recent review articles.[8,9,14,15] Section 2 discusses the materials physics of solution-processible p- and n-type organic semicon-

Henning Sirringhaus is the Hitachi Professor of Electron Device Physics at the Cavendish Laboratory. He has been working in the field of organic transistor devices since 1997. He has an undergraduate and Ph.D. degrees in physics from ETH Zürich (Switzerland). From 1995–1996 he worked as a postdoctoral research fellow at Princeton University (USA) on a-Si TFTs for active-matrix liquid crystal displays. His current research interests include the charge-transport physics of molecular and polymeric semiconductors, the development of printing-based nanopatterning techniques, and the use of scanning probe techniques for electrical characterization of functional nanostructures. He is co-founder and Chief Scientist of Plastic Logic Ltd., a technology start-up company commercializing printed organic transistor technology. He was awarded the Balzers Prize of the Swiss Physical Society in 1995 for his Ph.D. work on ballistic-electron-emission microscopy of epitaxial metal/semiconductor heterointerfaces, and the Mullard award of the Royal Society in 2003.

ADVANCED MATERIALS

ductors and dielectrics. Section 3 focuses at a more fundamental level on the electronic structure of solution-processed organic semiconductors and the charge-transport processes at the active interface, and how these are affected by disorder and molecular-relaxation effects. Finally, in Section 4 we review the current understanding of electronic-defect states and degradation mechanisms in OFETs, which lead to device instabilities and threshold-voltage (V_T) shifts upon bias stressing and/or environmental exposure.

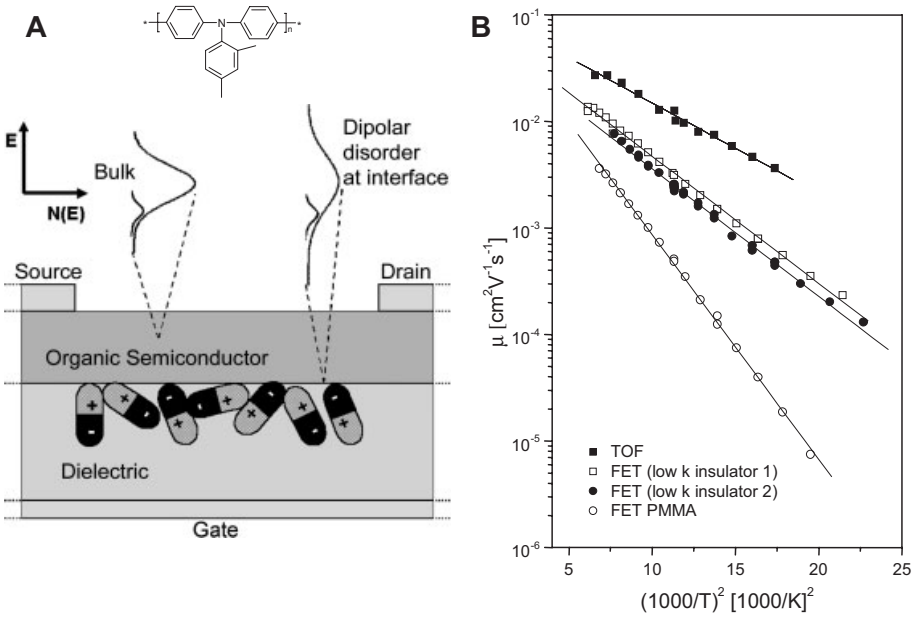

Figure 2. A) Schematic diagram of the effect of disordered polar groups on the energetic disorder at the active interface. B) Temperature (T) dependence of the time-of-flight (TOF) and field-effect mobility (μ) of PTAA. For the field-effect mobility data for top-gate FETs, a poly(methyl metacrylate) (PMMA) gate dielectric and two different lower-k dielectrics are shown.

2. Materials Physics

2.1. p-Type Semiconducting Polymers

Two different approaches to high-performance, solution-processible polymer semiconductors have emerged. The first approach is based on achieving high charge-carrier mobilities by designing the material to exhibit microcrystalline[16] or liquid-crystalline[17] order through self-organization, or by making use of specific interactions with a templating substrate. The second approach aims to produce a completely amorphous microstructure to provide a uniform path for charge transport, along which carriers experience a minimum degree of site-energy fluctuations. Although the first approach is likely to lead to higher mobilities eventually, impressive device performance and stability has been demonstrated with the second approach recently.

2.1.1. Amorphous Polymers

Early FET studies on amorphous, disordered, conjugated polymers, such as regioirregular polythiophene[4] or polyacetylene,[18] suggested that field-effect mobilities in amorphous microstructures might be limited to low values ($< 10^{-3}$–10^{-4} cm^2 V^{-1} s^{-1}). However, recently, several groups have reported that amorphous polymers based on triarylamine, similar to those used in xerographic applications, allow the achievement of high field-effect mobilities of 10^{-3}–10^{-2} cm^2 V^{-1} s^{-1}, combined with good operating, environmental, and photostability. Veres et al. have reported high-performance FETs with field-effect mobilities of up to 6×10^{-3} cm^2 V^{-1} s^{-1}, low threshold voltages, and good device stability based on a range of polytriarylamine (PTAA) derivatives.[19,20] These are used in combination with apolar, low-k polymer dielectrics (Fig. 2). With structurally related (9,9-dialkylfluorene-*alt*-triarylamine) (TFB) in contact with the benzocyclobutene dielectric, very stable device operation during continuous switching at 120 °C without device degradation was demonstrated.[21]

2.1.2. Microcrystalline Polymers

A prototype microcrystalline polymer is regioregular poly(3-hexylthiophene) (P3HT),[22,23] with which high field-effect mobilities of 0.1–0.3 cm^2 V^{-1} s^{-1} have been achieved. Thin films of P3HT adopt a highly microcrystalline and anisotropic lamellar microstructure comprising two-dimensional conjugated layers with strong π–π interchain interactions separated by layers of solubilising, insulating side chains (Fig. 3A); this microstructure leads to fast in-plane charge transport.[16] The microcrystals have been found to have a nanoribbon shape.[24–28] The mobility of P3HT depends very sensitively on the degree of head-to-tail regioregularity[22,23] and deposition conditions.[16,22,29] There is clear evidence, such as, for example, from studies of high-molecular-weight P3HT films with varying degrees of crystallinity as induced by varying the boiling point of the solvent,[27] that a higher degree of crystallinity generally results in higher mobility. The mobility has also been reported to increase with increasing molecular weight.[25] This has been attributed to grain boundaries limiting the transport in low-molecular-weight samples by Kline et al.,[25] while Zen et al.[30] have explained a similar observation in terms of a less planar polymer backbone in the amorphous regions of the film in the case of low-molecular-weight fractions. The mobility of P3HT FETs has also been reported to improve by orders of magnitude upon modification of the SiO_2

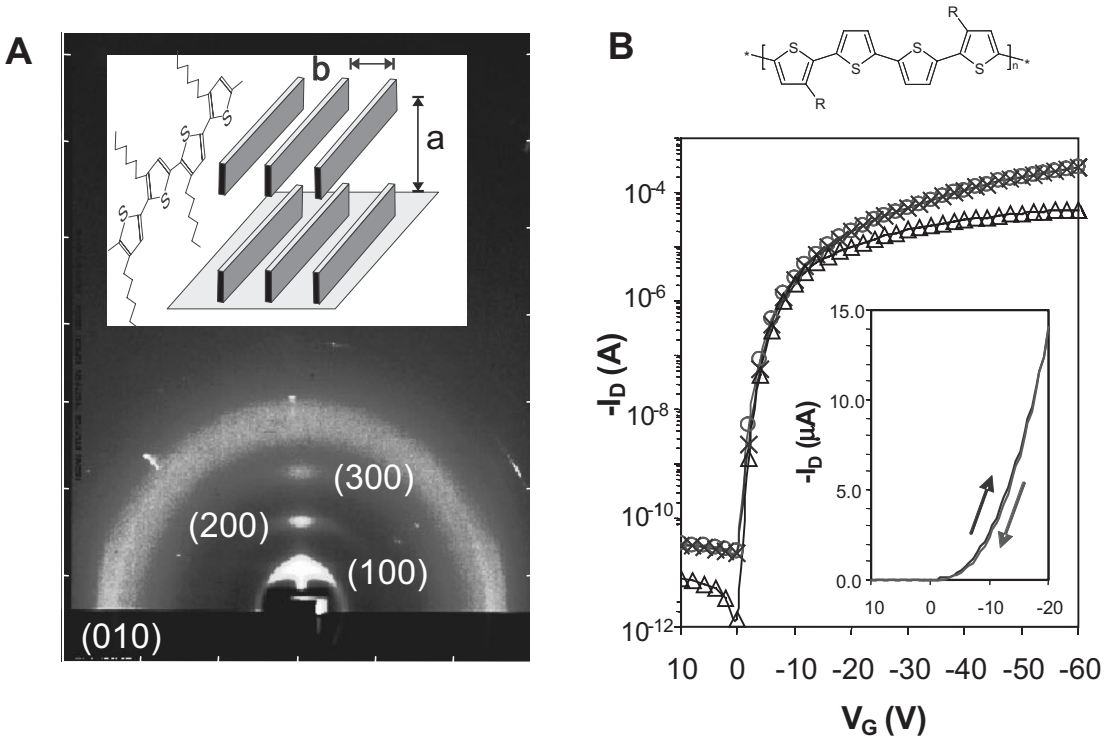

Figure 3. A) Wide-angle X-ray scattering image of high-mobility P3HT on SiO_2. The inset shows the in-plane, lamellar self-organisation of P3HT (*a* and *b* are lattice parameters). (Reprinted with permission from [16]. Copyright 1999, Nature Publishing Group.) B) Transfer characteristics (gate voltage, V_g, vs. drain current, I_d) of bottom-gate, top-contact poly(3,3‴-dialkylquaterthiophene) (structure shown) FET on SiO_2 measured unencapsulated under atmospheric conditions in the dark. (Reprinted with permission from [36]. Copyright 2004, American Chemical Society.)

gate dielectric substrate by hydrophobic self-assembled monolayers (SAMs), possibly through lowering of the surface energy of the gate dielectric and removal of residual surface water and other polar groups prior to deposition of the polymer,[23] or by inducing microstructural changes through specific interactions with functional groups of the polymer.[31]

p-Type semiconducting materials with low ionization potentials (typically less than 4.9–5.0 eV), such as regioregular P3HT, tend to exhibit large positive V_T shifts upon exposure to air, presumaby due to doping of the polymer.[32] P3HT is known to form a reversible charge-transfer complex with oxygen.[33] Nevertheless, encouraging shelf-life stability, albeit with a low ON/OFF current ratio of $< 10^3$, has been reported for P3HT FETs in a top-gate configuration, which may provide some encapsulation.[34] P3HT has poor photostability when exposed to ultraviolet sunlight in the presence of oxygen, causing formation of carbonyl defects in the polymer with associated loss of conjugation and mobility degradation.[35]

The oxidative stability of P3HT can be improved by increasing the ionisation potential of the polythiophene backbone by either disrupting its ability to adopt a fully planar conformation through the side-chain substitution pattern[36] or by incorporating partially conjugated co-monomers into the main chain.[37] These materials maintain the beneficial microcrystalline, lamellar self-organisation motive of the parent P3HT polymer and, as a result, exhibit similar field-effect mobilities but have significantly improved environmental and operating stabilities (Fig. 3B).

2.2. Solution-Processible Small Molecules

An alternative route to solution-processible organic semiconductors is to use small-molecule semiconductors that have been designed to be compatible with solution deposition.

2.2.1. Precursor Routes

Polycrystalline thin films of a conjugated molecule can be obtained by forming a thin film of a soluble precursor on the substrate with subsequent thermal[38] or irradiative[39] conversion into the fully conjugated form. Pentacene precursors have been shown to yield field-effect mobilities of 0.01–0.1 $cm^2 V^{-1} s^{-1}$[40] and 0.1–0.8 $cm^2 V^{-1} s^{-1}$[41] after thermal conversion at 150–200 °C. A precursor-route approach to tetrabenzoporphyrin has also been developed,[42] which yields a field-effect mobility on SiO_2 of 0.017 $cm^2 V^{-1} s^{-1}$ when converted at a temperature of 150–200 °C. Sexithiophene substituted with ester groups, which can be removed by thermolysis at 150–260 °C, exhibits field-effect mobilities on SiO_2 of up to 0.07 $cm^2 V^{-1} s^{-1}$.[43]

ADVANCED MATERIALS

2.2.2. Side-Chain Substitution

Small-molecule organic semiconductors can also be rendered solution processible by attachment of flexible side chains. The substitution pattern needs to be designed carefully such that the side chains that are needed to impart adequate solubility and film-forming properties do not interfere with the ability of the molecule to π-stack. Katz reported semiconductors of side-chain-substituted small molecules, such as dihexylanthradithiophene,[14,44] that can be solution-deposited with mobilities of 0.01–0.02 $cm^2 V^{-1} s^{-1}$. In bis(hexylbithiophene)benzene solution cast onto a heated SiO_2 substrate, mobilities of up to 0.03 $cm^2 V^{-1} s^{-1}$ were reported.[45] Due to the relatively low solubility of these molecules, growth conditions need to be optimized carefully to prevent aggregation and crystallization of the molecules in solution, which can lead to three-dimensional film morphology with poor connectivity and orientation of the grains in the films.

An interesting new strategy to solution-processible small conjugated molecules, such as rubrene, has recently been reported.[46] The approach is based on forming a eutectic mixture of the molecule with a vitrifying agent that suppresses crystallization in the as-deposited films. During rapid thermal annealing at a temperature above the melting temperature of the vitrifying agent crystallization of the molecule is induced, leading to large grain sizes and mobilities above 0.1 $cm^2 V^{-1} s^{-1}$.

2.2.3. Liquid-Crystalline Molecules

Side-chain-substituted small molecules, which exhibit liquid-crystalline phases at elevated temperatures, provide alternative routes to forming highly crystalline thin films from solution. Discotic liquid-crystalline molecules, such as hexabenzocoronenes, have been uniaxially aligned in thin-film form with the columnar axis oriented along the transport direction in the FET, by using graphoepitaxy on highly crystalline teflon alignment layers[47] or deposition by zone crystallization,[48] and have field-effect mobilities up to 0.01 $cm^2 V^{-1} s^{-1}$ along the discotic columns. Reactive mesogens, based on oligothiophenes with photopolymerizable end groups, have been homeotropically aligned on a substrate prior to crosslinking to fix the orientation of the molecules and used as the active FET layer.[49]

2.3. n-Type Semiconductors

Many organic semiconductors show p-type conduction only, i.e., in contact with a SiO_2 gate dielectric, for example, hole accumulation layers can be readily formed for negative gate bias, provided that a source–drain metal with a work function matching the ionization potential of the organic semiconductor is used. However, n-type organic semiconductors that exhibit electron transport in contact with a source–drain metal of suitably low work function upon application of positive gate bias are comparatively rare but are needed for realization of complementary logic circuits. Electron field-effect conduction has been reported in several, relatively high electron affinity (EA > 3.5 eV) small-molecule organic semiconductors deposited from the vacuum phase (see the review by Dimitrakopoulos et al.[13]) and solution-processed organic semiconductors. High-EA materials are less susceptible to the presence of electron-trapping impurities, since such trapping groups are more likely to be positioned, in energy terms, above the lowest unoccupied molecular orbital (LUMO) states of the organic semiconductor. It has been shown recently[50] (see Sec. 2.4) that electron conduction is, in fact, a generic feature of most organic semiconductors, including those with normal electron affinities of 2.5–3.5 eV, provided that the right dielectric, which avoids trapping of electrons at the interface, is used.

Fluoroalkyl-substituted naphthalenetetracarboxylic diimide can be processed into thin films from fluorinated solvents to yield mobilities of 0.01 $cm^2 V^{-1} s^{-1}$ (bottom-gate FET with SiO_2 dielectric and gold contacts).[51] The ladder polymer poly(benzobisimidazobenzophenanthroline) (BBL) has an electron affinity of 4.0–4.4 eV, and can be solution-processed into microcrystalline thin films from Lewis and methanesulfonic acids.[52] High electron mobilities of 0.03–0.1 $cm^2 V^{-1} s^{-1}$ were achieved in a bottom-gate FET configuration with SiO_2 dielectric measured unencapsulated in air. Solution-processed diperfluorohexyl-substituted quinque- and quaterthiophene with electron affinities of 2.8–2.9 eV have been reported to exhibit field-effect mobilties of $4–8 \times 10^{-4}$ $cm^2 V^{-1} s^{-1}$ (on HMDS-treated (HMDS: hexamethyldisilazane) SiO_2 dielectric with gold contacts). The devices suffer from a relatively high threshold voltage > 25 V due to electron trapping, which might be related to the relatively low electron affinity of fluoroalkyl-substituted thiophene molecules.[53] n-Type field-effect conduction has also been reported in methanofullerene phenyl C_{61}-butyric acid methyl ester (PCBM).[54] Field-effect mobilities of $3–4 \times 10^{-3}$ $cm^2 V^{-1} s^{-1}$ were achieved in an encapsulated, bottom-gate device with an organic dielectric and calcium source–drain contacts. Much lower apparent mobilities were observed with gold or aluminium contacts.

Recently, there has been growing interest in ambipolar organic semiconductors, which, in a device with a suitable choice of source–drain contacts, exhibit hole accumulation for negative gate bias and electron accumulation when the gate bias is reversed. One application of ambipolar semiconductors is in light-emitting FETs, which are operated by biasing the gate voltage in between the values of the source and the drain voltage to form a hole accumulation layer near the source contact and an electron accumulation layer near the drain contact. Ambipolar conduction was established in blends of solution-processed hole- and electron-transporting organic semiconductors by Meijer et al, using blends of hole-transporting poly(methoxy dimethyloctyloxy)-phenylene vinylene (OC_1C_{10}-PPV) or P3HT, with electron-transporting PCBM. The electron mobility in such blends (7×10^{-4} $cm^2 V^{-1} s^{-1}$) was two orders of magnitude lower than the electron mobility of a pure film of PCBM, while the hole mobility was similar to that

of single-component OC_1C_{10}-PPV (3×10^{-5} $cm^2\,V^{-1}\,s^{-1}$).[55] Similarly, Babel et al. reported ambipolar conduction measured in air in blends of BBL and CuPc (CuPc: copperphthalocyanine).[56] Also in this case, the electron (1.7×10^{-4} $cm^2\,V^{-1}\,s^{-1}$) and hole mobilities (3×10^{-5} $cm^2\,V^{-1}\,s^{-1}$) were several orders of magnitude lower than those of films of the single components. Interestingly, it was possible to improve either the electron or the hole mobility by post-deposition annealing under a solvent atmosphere; however, this was associated with the loss of the ambipolar conduction. Ambipolar conduction has also been reported in single-component systems such as low-bandgap poly(3,9-di-*tert*-butylindeno[1,2-*b*]fluorene) (PIF)[55] and soluble oligothiophene/fullerene donor–acceptor triads.[57]

2.4. Dielectrics

The performance of organic field-effect devices depends critically on the use of high-performance dielectrics that form active interfaces with low defect densities. In the same way as silicon metal oxide semiconductor (MOS) technology owes much to the quality of the Si/SiO_2 interface, dielectrics for organic FETs have recently received significant attention (see the comprehensive review by Facchetti et al.[58]). In comparison to inorganic heterointerfaces, many aspects of the physics of charge transport along solution-processed heterointerfaces are still poorly understood. In the present section we will review recent progress in the understanding of these issues and some of the general selection criteria for gate-dielectric materials.

For a solution-processed active interface, in which either the gate-dielectric material is deposited from solution onto a solution-processible semiconducting material or vice versa, it is critical to avoid dissolution or swelling effects during deposition of the upper layer, which can lead to interfacial mixing and increased interface roughness. This can be avoided by crosslinking the lower layer, restricting, however, the choice of materials and requiring special care to avoid introducing unwanted impurities and trapping groups.[59] The preferred approach is to choose orthogonal solvents for the deposition of the multilayer structure.[60] It has been demonstrated that in this way solution-processed interfaces can be achieved, at which the field-effect mobility is as high as that of the corresponding organic semiconductor/SiO_2 interface, for which interfacial mixing is not an issue.

This is somewhat surprising since a solution-processed polymer heterointerface is never atomically abrupt with its width being determined by a balance between entropy favoring a wider interface and the unfavorable energy of interaction between the two polymers.[61] The correlation between interface roughness and mobility in solution-processed OFETs has recently been investigated by Chua et al.,[62] who developed an approach for fabricating self-assembled polymer semiconductor–polymer dielectric bilayers making use of vertical phase separation in ternary solutions of the semiconducting polymer, gate-dielectric, and solvent. By varying the speed of solvent removal the roughness of the phase-separated interface could be varied in a controlled way. The mobility was found to be constant for low values of the interface roughness less than a critical roughness threshold. For roughness exceeding this threshold, a very rapid drop of the mobility by orders of magnitude was observed, even for roughness features of surprisingly long wavelength > 100 nm (Fig. 4).

In principle, for a given thickness of dielectric, a high-*k* dielectric is preferable to a low-*k* dielectric for an FET application that requires the FET to exhibit a high drive current at low drive voltage. Various solution-processible high-*k* dielectrics for low-voltage OFETs have been used in the literature, such as anodized Al_2O_3[63] (dielectric constant, $\breve{\alpha}$= 8–10), or TiO_2[64] ($\breve{\alpha}$= 20–41) (see the review by Veres et al.[20]). Low-voltage operation has also been achieved with very thin, sub-20 nm organic dielectrics, including SAM dielectrics,[65] SAM multilayers,[66] or ultrathin polymer dielectrics.[21] Many polar, high-*k* polymer dielectrics, such as polyvinylphenol ($\breve{\alpha}$= 4.5) or cyanoethylpullulan ($\breve{\alpha}$= 12), are hygroscopic and susceptible to drift of ionic impurities during device operation and cannot be used for ordinary TFT applications.[67]

Veres et al. have shown that the field-effect mobilities of amorphous PTAA[19] and other polymers[20] are higher when those materials are in contact with low-*k* dielectrics with $\breve{\alpha}$ < 3 than with dielectrics with higher *k*. The latter usually contain polar functional groups, which are randomly oriented near the active interface; this is believed to increase the energetic

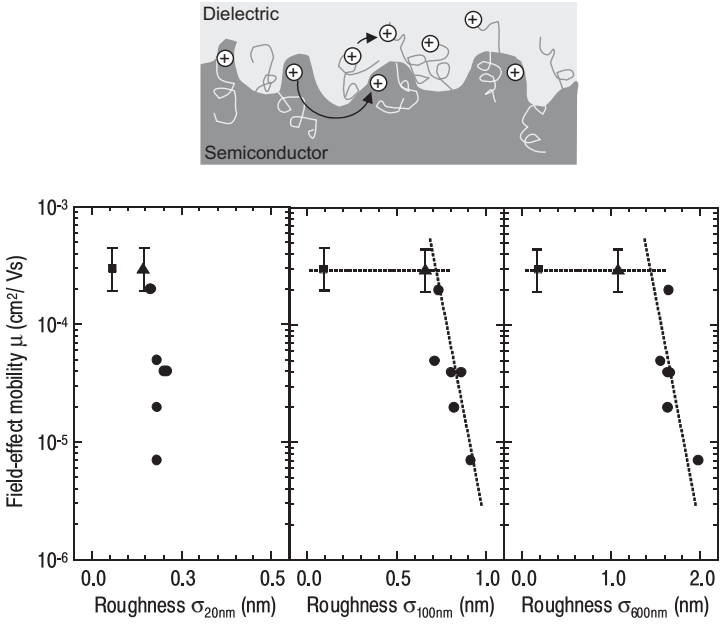

Figure 4. Schematic diagram of the interface structure at a solution-processed polymer/polymer heterointerface, and correlation between mobility and interface roughness on different length scales obtained from a series of self-assembled bilayer FETs based on TFB/BCB (BCB: benzocyclobutene).

disorder at the interface beyond what naturally occurs due to the structural disorder in the organic semiconductor film itself, resulting in a lowering of the field-effect mobility (Fig. 2A). Low-*k* dielectrics also have the advantage of being less susceptible to ionic impurities, which can drift under the influence of the gate field, causing device instabilities (see Sec. 4).

The chemical purity and composition of the gate dielectric can have dramatic effects on interfacial charge transport. The reason for the absence of n-type field-effect conduction in "normal" polymers, such as poly(*p*-phenylenevinylene)s (PPVs) or P3HT, with electron affinities of around 2.5–3.5 eV has puzzled the community for some time because in LED devices many of these polymers support electron conduction. Chua et al.[50] have demonstrated that by using appropriate gate dielectrics that are free of electron-trapping groups, such as hydroxyl, silanol, or carbonyl groups, n-channel FET conduction is in fact a generic property of most conjugated polymers. In contact with trapping-free dielectrics, such as benzocyclobutene, BCB, which are free of functional groups such as hydroxyl groups that have an electron affinity larger than that of the organic semiconductor used, electron and hole mobilities were found to be of comparable magnitude in a broad range of polymers. Some polymers, such as P3HT and OC_1C_{10}-PPV, even exhibit ambipolar charge transport in suitable device configurations (Fig. 5), which demonstrates clean inversion behavior in organic semiconductors with bandgaps >2 eV. The reason why n-type behavior has previously been so elusive is that most studies were performed on SiO_2 gate dielectrics, for which electrochemical trapping of electrons by silanol groups at the interface occurs.[50]

3. Electronic Structure and Charge-Transport Physics of Polymer Semiconductors

3.1. Electronic Structure

The electronic structure of conjugated-polymer semiconductors reflects the complex interplay between intrinsic π-electron delocalization along the polymer backbone and strong electron–phonon coupling, and the existence of energetic and positional disorder in solution-processed thin films. In a hypothetical, infinitely straight polymer chain, the highest occupied molecular orbital (HOMO) and LUMO states of the neutral polymer are fully delocalized along the polymer chain and exhibit, in fact, significant dispersion with calculated bandwidths of several electron volts.[68] However, as a result of the strong electron–phonon coupling and the disorder-induced finite conjugation length, charges introduced onto the polymer interact strongly with certain molecular vibrations and are able to lower their energy with respect to the extended HOMO/LUMO states by forming localized polarons surrounded by a region of molecular distortion.[69] There

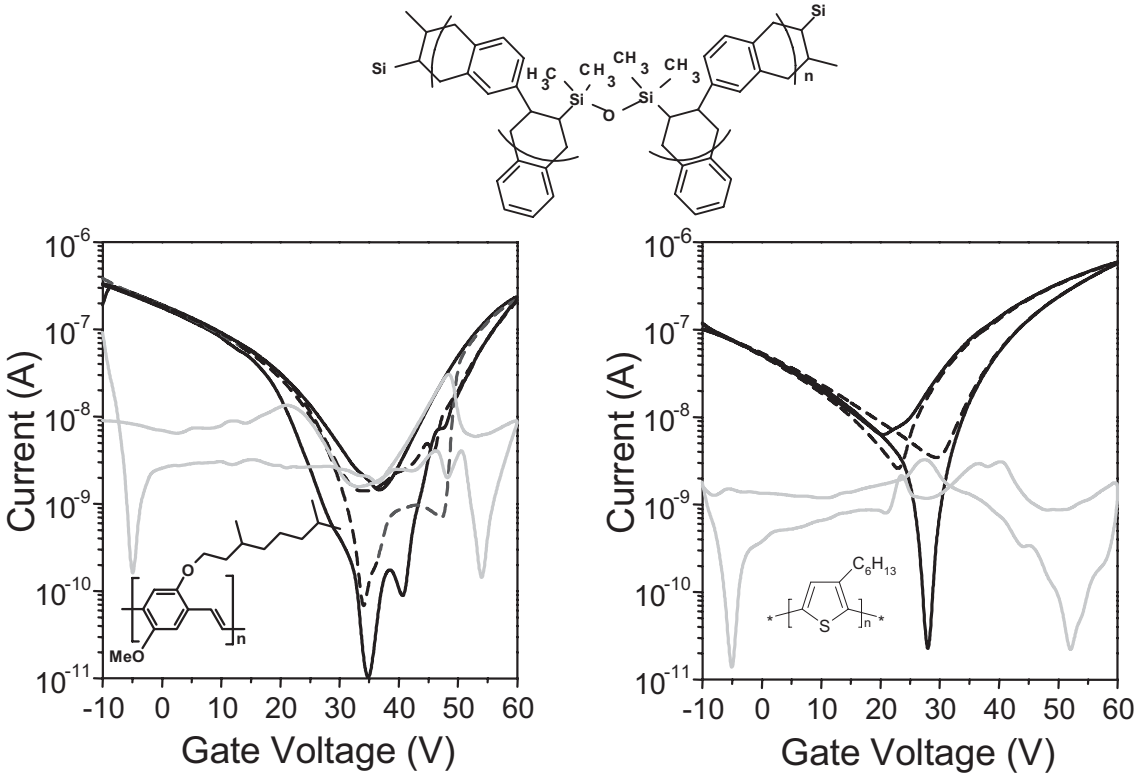

Figure 5. Transfer characteristics of bottom-gate OC_1C_{10}-PPV (left) and P3HT (right) FETs with trap-free BCB (structure shown) gate dielectrics exhibiting clean ambipolar transport ($V_{sd} = 60$ V). Grey lines: gate leakage current. (Courtesy of Jana Zaumseil, University of Cambridge).

is clear, experimental evidence that the charge carriers carrying the current in a conjugated-polymer FET are indeed of polaronic nature. Due to the surrounding molecular distortion and electronic relaxation, the charged molecule exhibits characteristic optical transitions below the absorption edge of the neutral molecule. These can be observed in operational FETs using charge-modulation spectroscopy (CMS), which detects changes of the optical transmission of a semitransparent FET device upon gate-voltage-induced modulation of the carrier concentration in the accumulation layer.[70]

In polymers, such as poly(dioctylfluorene-*co*-bithiophene) (F8T2), in which close interchain interactions are weakened by the sp^3-coordinated carbon atom on the fluorene unit, there are two characteristic sub-bandgap polaronic absorptions, which can be accounted for by the dipole-allowed C1 (≈ 0.4 eV) and visible C2 (1.6 eV) transitions of a simple isolated chain model (Fig. 6A).[71] In contrast, the charge-induced absorption spectrum of P3HT (Fig. 6B) can only be explained by taking into account interchain interactions.[72] In addition to the C1 (0.3 eV) and C2 (1.3 eV) transitions, the CMS spectrum of high-mobility P3HT exhibits an additional C3 transition (1.6–1.8 eV), which is dipole-forbidden in the isolated-chain case and low-energy, charge-transfer (CT) transitions at 60–120 meV.[16,73] Polarons in P3HT are not confined to a single chain, but are spread over several, π-stacked chains. As a result of their two-dimensional nature the polaron binding energy in P3HT is much reduced. From the position of the CT transition (E_{CT}),[69] the polaron binding energy, E_p, can be estimated to be on the order of $E_p \approx E_{CT}/2 \approx 30$–$60$ meV.

3.2. Charge Transport

At sufficiently high temperatures, charge transport of polaronic carriers in conjugated polymers should be governed by the physics of electron-transfer processes, which was established by Marcus for chemical reactions and biological electron-transfer processes.[74] In order for the localized polaron to hop between neighboring sites, the molecular configurations of the initial (occupied) site and the final (empty) site need to be distorted to a common configuration, where the molecular distortion of both sites is equal (configuration B in Fig. 7B). This leads to thermally activated transport even in the absence of disorder. In the non-adiabatic limit, where the timescale for electron hopping is longer than that of the lattice vibrations, the mobility is given by:

$$\mu = \frac{ea^2}{k_B T} \nu \exp\left(-E_p / 2k_B T\right) \quad (1)$$

where e is the electronic charge, a is the typical hopping distance, k_B is Boltzmann's constant, T is temperature, and ν is the attempt frequency:

$$\nu = \frac{\sqrt{\pi} J^2}{\hbar \sqrt{2 E_p k_B T}} \quad (2)$$

where J is the nearest-neighbor interaction energy and $\hbar$ is Planck's constant.

However, in most experimental systems the manifestations of the polaronic character of the charge carriers are masked by the effects of disorder. In any solution-deposited thin film

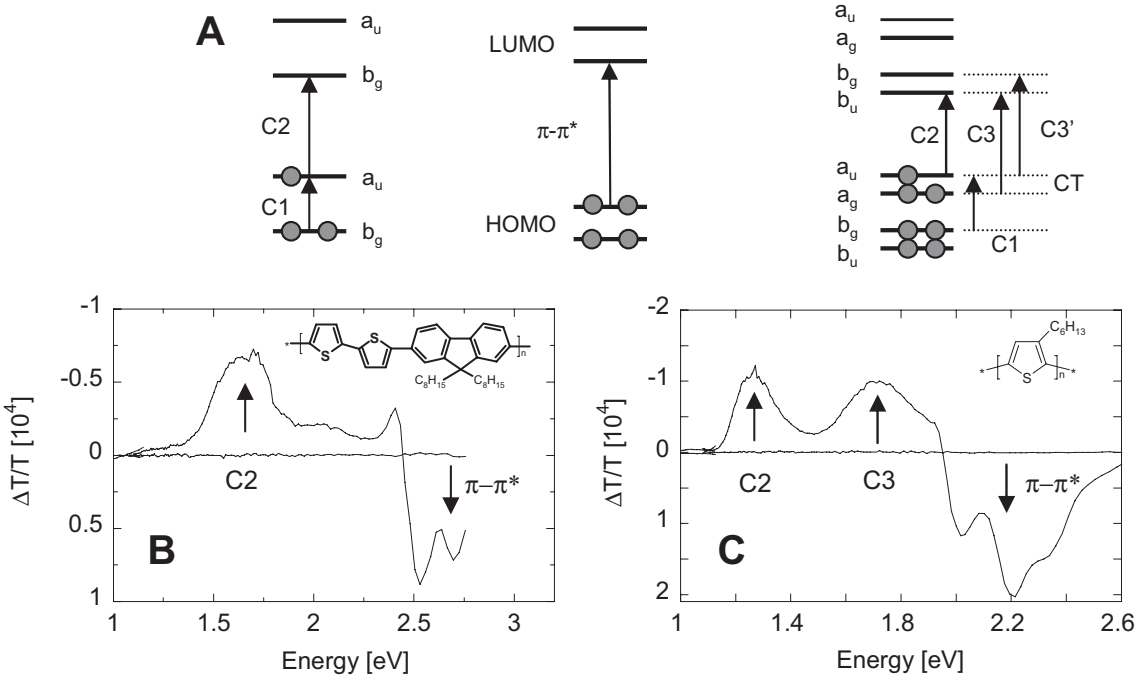

Figure 6. A) Schematic energy diagram of a neutral polymer (center), polaronic absorptions in the case of isolated chains (left), and interacting chains (right); B,C) Charge modulation spectra of F8T2/PMMA and P3HT/PMMA top-gate FETs, respectively (Courtesy of Shalom Goffri, University of Cambridge).

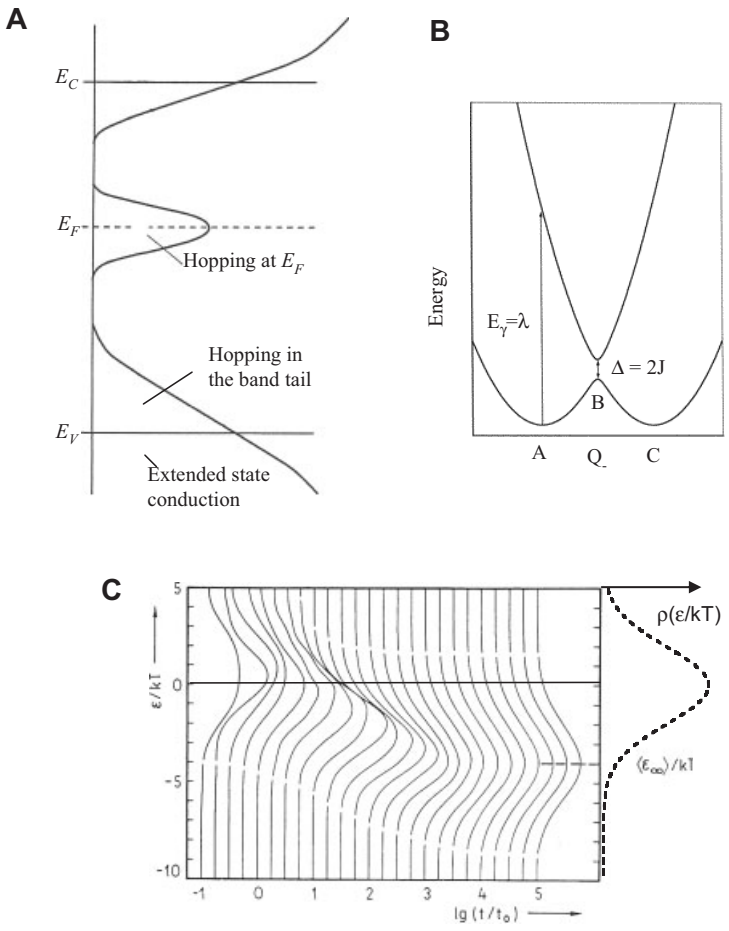

Figure 7. A) Schematic energy diagram (E_C, E_F, E_V are the conduction band, valence band, and Fermi energies, respectively) of density of states (DOS) of a disordered semiconductor with a mobility edge. B) Potential-energy diagram as a function of configuration coordinate, illustrating polaron hopping motion between two sites A and C through a coincidence configuration B. The transition energy λ for optically induced charge transfer is also indicated (Q_: configuration coordinate). C) Relaxation of energy distribution of an injected charge-carrier hopping in a Gaussian DOS as a function of time (t). The DOS is shown as a dashed line on the right.

disorder is present and causes the energy of a polaronic charge carrier on a particular site to vary across the polymer network. Variations of the local conformation of the polymer backbone, presence of chemical impurities or structural defects of the polymer backbone, or dipolar disorder due to random orientation of polar groups of the polymer semiconductor or the gate dielectric result in significant broadening of the electronic density of states.

The transport of charges injected into a molecular solid dominated by the effects of disorder is well understood from the work on molecularly doped polymers and other organic photoconductors used in xerography. Assuming a disorder-broadened Gaussian density of transport states with a characteristic width σ, Bässler[75] has shown on the basis of Monte Carlo simulations that an injected carrier hopping through such an otherwise empty density of states (DOS) relaxes to a dynamic equilibrium energy, $\langle\check{\alpha}_{\sim\infty}\rangle = -\sigma^2/kT$, below the center of the DOS (Fig. 7C) leading to a characteristic $\log\mu \propto 1/T^2$ temperature dependence of the mobility. The model has been improved by Novikov et al.,[76] who showed that the dominant source of diagonal disorder is due to charge–dipole interactions, and that spatial correlations of such interactions need to be taken into account in order to explain the commonly observed Poole–Frenkel dependence of the mobility on the electrical field, and who derived an expression for the electric-field (E) and temperature dependence of the mobility in a correlated DOS with both diagonal as well as non-diagonal, positional disorder:

$$\mu = \mu_0 \exp\left[-\left(\frac{3\sigma}{5k_B T}\right)^2 + 0.78\left(\left(\frac{\sigma}{k_B T}\right)^{3/2} - 2\right)\sqrt{\frac{eaE}{\sigma}}\right] \quad (3)$$

The model describes the transport of individual injected carriers at zero/small carrier concentrations, i.e., it should in principle not be directly applicable to the relatively high carrier concentrations $p = 10^{18}$–10^{19} cm^{-3} present in the accumulation layer of FETs. Vissenberg and Matters[77] have developed a percolation model for variable-range hopping transport in the accumulation layer of an FET assuming an exponential DOS with width T_0. An expression for the field-effect mobility as a function of carrier concentration p was derived:

$$\mu_{FE} = \frac{\sigma_0}{e}\left[\frac{\left(\frac{T_0}{T}\right)^4 \sin\left(\pi\frac{T}{T_0}\right)}{(2a)^3 B_c}\right]^{T_0/T} p^{\frac{T_0}{T}-1} \quad (4)$$

where σ_0 is the prefactor for the conductivity, a is the effective overlap parameter between localized states, and $B_c \simeq 2.8$ is the critical number for onset of percolation. Transport in this model can be effectively described as activation from a gate-voltage-dependent Fermi energy to a specific transport energy in the DOS.

Tanase et al.[78] have shown that in a series of isotropic, amorphous PPV polymers the large difference between the low mobility values extracted from space-charge-limited current measurements in LEDs and the comparatively higher field-effect mobilities can be explained by the largely different charge-carrier concentrations (Fig. 8). It was possible to fit the temperature dependence of the zero-field LED mobility to Equation (3), and the carrier-concentration dependence of the FET mobility to Equation (4) with a consistent value of $\sigma = 93$–125 meV. The gate-voltage dependence of the FET mobility of MEH-PPV (poly(2-methoxy-5-(2′-ethylhexyloxy)-1,4-phenylenevinylene)) has also been analysed by Shaked et al.[79]

In several higher-mobility, amorphous, hole-transporting materials, such as PTAA,[19] TFB,[21] as well as in nematic,

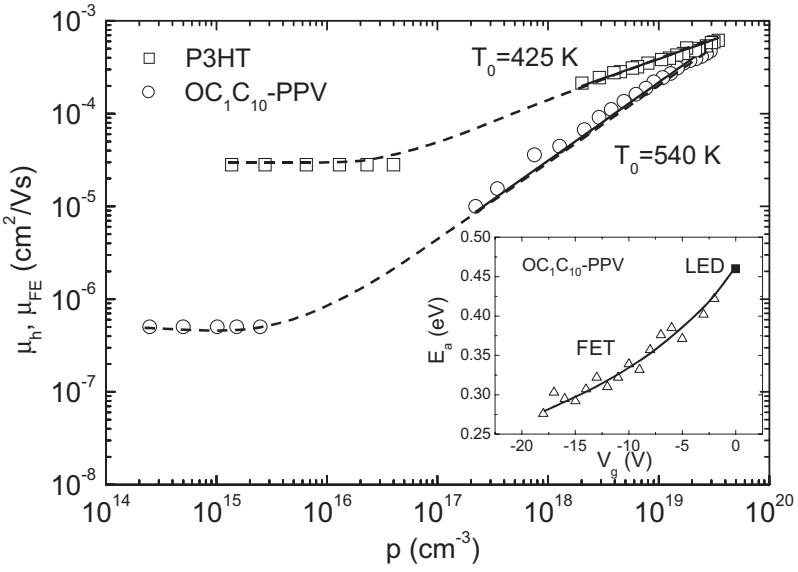

Figure 8. Hole mobility (μ_h) as a function of charge-carrier concentration (p) in diode and field-effect transistors for P3HT and a PPV derivative, respectively. The inset shows the temperature activation energy of the mobility as a function of gate voltage. (Reprinted with permission from [78]. Copyright 2003, American Physical Society.)

glassy polyfluorene-*co*-bithiophene,[17] a somewhat different behavior was observed. The field-effect mobility was found to be independent of gate voltage within the carrier concentration range 10^{18}–10^{19} cm^{-3}. In PTAA, the low-density time-of-flight (TOF) and high-density field-effect mobilities are of similar magnitude, with the bulk TOF mobility being even higher, by a factor of 2–3, at room temperature than the field-effect mobility. The Gaussian disorder model was used to extract significantly smaller values of $\sigma = 57$ meV and $\sigma = 68$–90 meV from the temperature dependence of the TOF and field-effect mobility of amorphous PTAA, respectively (Fig. 2B). The increased σ value in the case of the FET mobility was attributed to the contribution to energetic disorder from polar disorder in the dielectric close to the charge-transporting accumulation layer.

The reason for the different behavior observed in PPVs, with room-temperature field-effect mobilities of $<10^{-3}$–10^{-4} cm^2 V^{-1} s^{-1}, and the higher mobilities of PTAA and polyfluorene polymers ($\mu_{FET} = 10^{-3}$–10^{-2} cm^2 V^{-1} s^{-1}) might be related to the lower degree of energetic disorder in the latter. With a narrow DOS ($\sigma < 60$–90 meV), the expected concentration dependence of the room-temperature mobility over a concentration range 10^{14}–10^{19} cm^{-3} spanned by LED/FET measurements is relatively weak, i.e., less than an order of magnitude, and might be masked by other effects, such as differences in bulk and interface microstructure, effects of interface roughness, or disorder effects induced by polar or charged groups in the dielectric.

An alternative theoretical framework for understanding the effects of disorder is the multiple-trapping model, which is well established for describing transport in a-Si and has been claimed to be more appropriate for describing the charge transport in microcrystalline polymers, such asP3HT[23] and poly(bis(alkylthienylbithiophene).[80] This model assumes that disorder broadening is sufficiently weak that, in a certain energy range, the DOS becomes high enough so electronic states above the so-called mobility edge are extended, while electronic states below the mobility edge remain localized (Fig. 7A). The current is assumed to be transported by carriers that are thermally activated into the delocalized states above the mobility edge, while carriers in localized states are effectively trapped. Assuming a specific DOS and a mobility for carriers above the mobility edge, the FET current can be obtained by first determining the position of the quasi-Fermi level at the interface for a particular gate voltage and then calculating the number of free carriers that are thermally excited above the mobility edge using Fermi–Dirac statistics.

Salleo et al.[80] found that the multiple-trapping model explained the temperature dependence of the FET mobility of poly(bis(alkylthienylbithiophene) more consistently than the Vissenberg hopping model, the latter yielding an unphysical dependence of σ_0 and T_0 on the processing conditions. Similarly, in the author's experience, the gate-voltage dependence of P3HT cannot be fitted consistently in the framework of the Vissenberg model. Figure 9 shows temperature- and gate-voltage-dependent field-effect mobility data for P3HT obtained from scanning Kelvin probe microscopy (SKPM),[81] which provides a very accurate, local measurement of the field-effect mobility without being affected by contact resistance, non-uniform electric-field effects, etc., which complicate extraction of field-effect mobilities from device charac-

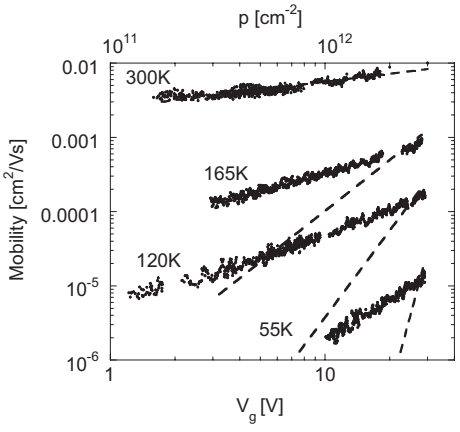

Figure 9. Field-effect mobility at the P3HT/SiO_2 interface as a function of gate voltage and temperature, extracted from scanning Kelvin probe microscopy (SKPM) measurements. The dashed lines show the gate-voltage dependence expected in the Vissenberg model using the value of T_0 extracted from the room-temperature data.

ADVANCED MATERIALS

teristics. From the fit of the room temperature data to Equation 4, a value of $T_0 = 353$ K is extracted. However, it is impossible to fit consistently the data over the temperature range with the same value of T_0. At low temperature the dependence of the mobility of P3HT on carrier concentration is much weaker than predicted by the variable-range hopping model.

It is intriguing to ask the question whether transport in the highest-mobility P3HT samples ($\mu > 0.1$ cm^2 V^{-1} s^{-1}) is limited entirely by disorder or to which degree the observed temperature-activated transport may reflect polaron hopping characteristics. Fishchuk et al.[82] derived a criterion to estimate whether polaronic contributions need to be taken into account when describing transport in a disordered organic semiconductor. In the framework of the Gaussian disorder model, for polaronic transport effects to be observable, the activation energy for polaron hopping, $E_p/2$, needs to be comparable to the expected transport activation energy due to disorder, $9\sigma^2/25k_BT$ (Eq. 4). Using the above values of E_p for P3HT as estimated from the position of the CT transition, the expected activation energy for polaron hopping of 15–30 meV is starting to become comparable to the observed activation energy of the field-effect mobility near room temperature for the highest-mobility P3HT samples (20–40 meV), implying that polaronic effects might need to be taken into account to explain the transport properties of high-mobility polymer semiconductors.[83]

3.3. Charge Injection

Another important aspect of the device physics, particularly in the context of short-channel OFETs with channel length $L < 5$ μm is the injection of charges from a metal source–drain contact into the organic semiconductor. In contrast to inorganic semiconductors, controlled doping of organic semiconductors is still difficult, since dopants incorporated in the form of small-molecule counterions can migrate and cause device instabilities. Since most organic semiconductors that have shown useful FET performance have bandgaps > 2 eV, the formation of low-resistance, ohmic contacts with common metals is often challenging.

One of the most direct and powerful methods for study of the injection physics in bottom-gate OFETs is SKPM, which provides a direct measurement of the voltage drop across the injecting contacts in an operational bottom-gate FET.[84–86] In normal FET operation, the source contact is reverse biased while the drain contact is forward biased, implying that the source-contact resistance should be significantly larger than the drain-contact resistance. It has been observed that in bottom-contact, bottom-gate devices with optimized Schottky barriers, Φ_b, less than 0.3 eV, such as P3HT/Au, the contact resistance at the source contact is in fact very similar to that at the drain contact. This implies that, under conditions that might be typical for high-performance OFETs, the contact resistance is not determined by the Schottky barrier at the interface but by bulk-transport processes in the semiconductor in the vicinity of the contact. Consistent with this interpretation, the contact resistance was found to depend on temperature in the same way as the mobility.[85] This result was explained by invoking the existence of a depletion layer in the vicinity of the contacts. Similar results have been reported using channel-length scaling analysis.[87]

In systems with Schottky barriers exceeding 0.3 eV, the source resistance was found to be larger than the drain resistance, as expected, implying that in this regime the contact resistance is determined by the injection physics at the interface.[85] It is remarkable that, in spite of the significant expected Schottky-barrier height, the contact resistance shows only a very weak increase with decreasing temperature, which is even weaker than that of the field-effect mobility (Fig. 10A). This behavior cannot be explained in the framework of the commonly used diffusion-limited thermionic emission model,[88] which takes into account back-scattering into the metal due to the small mean free path in the organic semiconductor and predicts the activation energy of the contact resistance to be larger than that of the mobility and larger than Φ_b/k_BT. Explanation of the experimental data required taking into account disorder-induced broadening of the DOS of the organic semiconductor, which provides carriers with injection pathways through deep states in the DOS, leading to a reduced effective barrier at low temperatures (Fig. 10B).

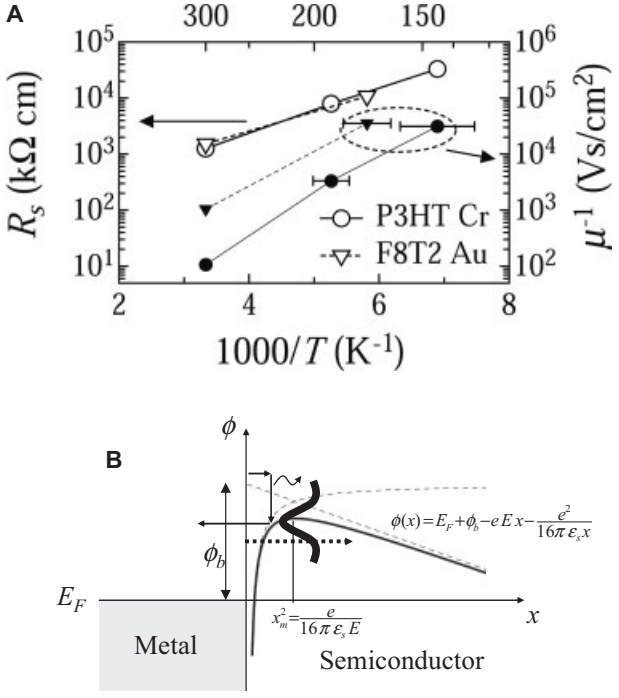

Figure 10. A) Comparison of the temperature (T) dependence of the contact resistance (R_S) and field-effect mobility of bottom-gate FETs of P3HT/SiO_2 or F8T2/SiO_2 with bottom-contact chromium or gold contacts, respectively. (Reprinted with permission from [85]. Copyright 2003, American Physical Society.) B) Schematic energy diagram of charge injection at the interface between a metal electrode (E_F is Fermi energy of metal contact) and a disordered, low-mobility organic semiconductor.

In most metal–semiconductor systems, the contact resistance for p-type injection increases sensitively with decreasing work function of the metal, although, in most cases, less strongly than expected from simple Mott–Schottky theory. One of the topics that warrants further study is a more detailed understanding of the role of chemical interactions between the metal and the organic semiconductor. Gold diffusion into pentacene has been made responsible for trap generation that limits contact injection into pentacene.[89] There are also intriguing reports of efficient charge injection in systems for which Schottky barriers, calculated using Mott–Schottky theory, should exceed 1 eV, such as hole injection from Ca into P3HT[50] or electron injection from Au into fluorocarbon-substituted oligothiophenes;[90] these results suggest that chemical interactions and interface states are important.

4. Degradation Mechanisms Causing Threshold-Voltage Instabilities

Electronic defect states in the semiconductor, at the interface between semiconductor and dielectric and inside the dielectric layer, can cause instabilities of the threshold voltage, V_T, of the TFT. For practical applications, the V_T stability is an as important, if not more important, figure of merit as the field-effect mobility, because it is closely related to the operational and shelf lifetimes of the device. Most TFT technologies, including those based on a-Si, suffer from V_T shifts induced by bias-temperature stress (BTS). In a-Si TFTs, both generation of defect states inside the semiconducting layer, such as dangling-bond defects, as well as charge injection into the SiN_x gate dielectric have been found to contribute to V_T shifts upon BTS, with charge injection into the dielectric being the dominant mechanism in high-quality material.[91] Several groups have recently reported systematic BTS investigations and studies of organic TFT characteristics upon exposure to atmospheric conditions and humidity.

In most p-type organic semiconductors a negative shift of the threshold voltage is observed upon prolonged operation of the device in accumulation, which is generally attributed to charge trapping in the organic semiconductor and/or at the active interface. Matters et al. reported negative V_T shifts due to charge trapping for a polythienylenevinylene (PTV) precursor polymer in contact with an inorganic SiO_2 dielectric, which were more pronounced in the presence of water than when the device was operated in vacuum or dry air.[92] Street et al. reported significant negative V_T shifts in F8T2/SiO_2 bottom-gate, bottom-contact TFTs,[93] which were more pronounced than reported for top-gate F8T2 devices with a polymer dielectric.[17] Those authors also found the V_T stability of PQT/SiO_2 devices to be significantly better than that of F8T2/SiO_2 devices. It is clear from these experiments, that the device configuration, choice of contacts, and dielectric play a crucial role in determining the device stability.

There is little known at present about the nature of the electronic states involved in defect formation and device degradation. Few experimental studies have been aimed at understanding at a microscopic level the nature of defect states in organic semiconductors.[94] Device modeling has been used to understand the subthreshold characteristics of OFETs.[95] Based on an analysis of the relationship between the current decay at the early stages after FET turn-on and the hole concentration in the channel, Street et al. have suggested that charge trapping occurs due to formation of low-mobility bipolarons by reaction of two polarons.[93,96] However, Deng et al. performed optical spectroscopy of field-induced charge on F8T2/PMMA TFTs exhibiting significant V_T shifts but were unable to detect the spectroscopic signature of bipolarons.[71]

Some of the negative V_T shift due to charge trapping can be recovered by not operating the device for time periods of several minutes or hours, by application of a positive gate bias, or by illuminating the sample with above-bandgap light[97,98] (Fig. 11A). In the latter case, electron–hole pairs are generated in the organic semiconductor in the vicinity of the trapped hole charge. The photogenerated electron has a chance of recombining with the trapped hole leaving behind a mobile positive hole. The spectral dependence of the light-induced recovery follows the absorption spectrum of the organic semiconductor (Fig. 11B). Charge traps that can be emptied in this way must be located inside the organic semiconductor or directly at the interface, but cannot be located inside the gate dielectric.

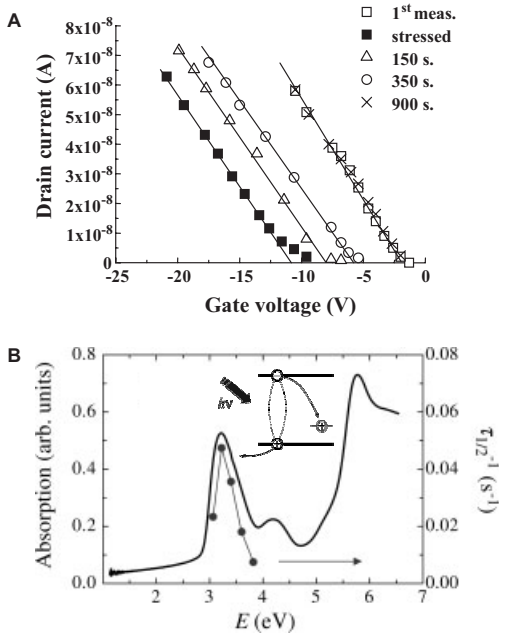

Figure 11. A) Pulsed transfer characteristics of a bottom-gate F8T2/SiO_2 FET after applying a negative gate bias stress. The subsequent recovery of the threshold-voltage shift after illuminating the device for different periods of time is shown. (Reprinted with permission from [97]. Copyright 2003, American Physical Society.) B) Comparison of the wavelength dependence of the time constant ($\tau_{1/2}$, full circles) for the light-induced trap release in TFB/SiO_2 with the absorption spectrum of the organic semiconductor (solid line). (Reprinted with permission from [98]. Copyright 2004, Elsevier.)

ADVANCED MATERIALS

It has also been reported that a positive gate voltage stress leads to a shift of V_T to more positive values.[97] This has recently been explained by injection and trapping of negative electrons at the interface.[50]

Zilker et al. have reported that in films of p-type, solution-processed pentacene in contact with an organic photoresist dielectric the threshold voltage shifts to more positive values for negative gate bias stress during operation in air.[99] The V_T shift was more pronounced the smaller the source–drain voltage. This was interpreted as being the result of mobile ions drifting in the gate dielectric in the presence of water. Negative ions drifting towards the active interface cause accumulation of positive countercharges in the semiconducting layer. Only during operation in vacuum or in dry air was a negative V_T shift of –3 V (after application of $V_g = -20$ V for 1000 s) observed, which resulted from charge trapping at or near the interface. Rep et al. have investigated the role of ionic impurities originating from the substrate on the conductivity of P3HT films.[100] On Na_2O-containing glass substrates, Na^+ ions were found to drift towards the negatively biased contact leaving behind negative charge centers on the glass surface.

The above results point to the crucial role of the gate dielectric in determining the operational and shelf stability of the device. Several groups have recently reported very encouraging BTS and shelf-lifetime data for solution-processed OFETs measured and stored in air without special encaspulation. PTAA combined with low-*k* dielectrics exhibit excellent shelf life with no discernible V_T shift upon storage in air and light for periods of several months.[19] Similarly, TFTs based on TFB with a BCB dielectric exhibit very good operational stability during accelerated lifetime testing at temperatures of 120 °C.[21] In both cases the good stability is believed to be related to the use of an apolar, low-*k* dielectric, which is less susceptible to ionic impurities, and to the amorphous microstructure of the arylamine-based polymer semiconductor, which has good thermal and photostability and a low degree of energetic disorder. The group at Plastic Logic has recently reported excellent operational-stability results on unencapsulated, polymer TFTs fabricated on poly(ethylene terephthalate) (PET) substrates.[11] Although there is still, of course, significant work to assess and improve the operational and shelf life of OFETs under realistic application conditions and to understand degradation mechanisms in much more detail, these results strongly suggest that solution-processed OFETs can exhibit similar device stability and reliability to their a-Si counterparts.

5. Outlook

Solution-processible organic FETs have become a promising emerging technology for low-cost, large-area electronics on flexible, plastic substrates. FET performance is approaching that of a-Si TFTs, and solution/printing-based manufacturing processes have been developed. Recently, device operational and environmental stabilities have improved significantly as a result of availibility of organic semiconductors with higher inherent oxidative stability, better understanding of the requirements for gate dielectrics, and more controlled manufacturing processes. In this article we have reviewed recent progress in understanding the device physics of solution-processible organic semiconductors. Unfortunately, due to space limitations some important work in this field could not be discussed. It should be apparent from the discussion that, although much progress has been made in understanding the materials physics and requirements for high performance FETs, our understanding of the fundamental excitations and processes at a microscopic level involved in charge transport and injection as well as device degradation is still much more superficial than the corresponding level of fundamental understanding available for inorganic semiconductors. In particular, many fundamental aspects of the correlation between the structure and physics of charge transport at solution-processed organic/organic heterointerfaces remain to be explored. However, the field of organic electronics is gaining momentum through continued breakthroughs in materials and device performances; concrete industrial applications of active-matrix flexible electronic-paper displays and simple, low-cost intelligent labels are emerging on the horizon to be commercialized within the next three to five years. As some of the recent work reviewed in this article will have shown, there is still ample room for fundamental, scientific discoveries, and the field is expected to remain exciting and stimulating for the foreseeable future.

Received: June 6, 2005
Published online: September 15, 2005

[1] G. H. Heilmeier, L. A. Zanoni, *J. Phys. Chem. Solids* **1964**, *25*, 603.
[2] G. Horowitz, X. Z. Peng, D. Fichou, F. Garnier, *Solid State Commun.* **1989**, *72*, 381.
[3] E. Ebisawa, T. Kurokawa, S. Nara, *J. Appl. Phys.* **1983**, *54*, 3255.
[4] H. Koezuka, A. Tsumara, T. Ando, *Synth. Met.* **1987**, *18*, 699.
[5] J. H. Burroughes, C. A. Jones, R. H. Friend, *Nature* **1988**, *335*, 137.
[6] P. F. Baude, D. A. Ender, M. A. Haase, T. W. Kelley, D. V. Muyres, S. D. Theiss, *Appl. Phys. Lett.* **2003**, *82*, 3964.
[7] I. McCulloch, presented at the 229th ACS Natl. Meeting, San Diego, CA, March 2005.
[8] H. Sirringhaus, L. Buergi, T. Kawase, R. H. Friend, in *Thin Film Transistors* (Eds: C. R. Kagan, P. Andry), Marcel Dekker, New York **2003**, p. 427.
[9] S. R. Forrest, *Nature* **2004**, *428*, 911.
[10] G. H. Gelinck, H. E. A. Huitema, E. Van Veenendaal, E. Cantatore, L. Schrijnemakers, J. Van der Putten, T. C. T. Geuns, M. Beenhakkers, J. B. Giesbers, B. H. Huisman, E. J. Meijer, E. M. Benito, F. J. Touwslager, A. W. Marsman, B. J. E. Van Rens, D. M. de Leeuw, *Nat. Mater.* **2004**, *3*, 106.
[11] K. Reynolds, S. Burns, M. Banach, T. Brown, K. Chalmers, N. Cousins, L. Creswell, M. Etchells, C. Hayton, K. Jacobs, A. Menon, S. Siddique, C. Ramsdale, W. Reeves, J. Watts, T. V. Werne, J. Mills, C. Curling, H. Sirringhaus, K. Amundson, M. D. McCreary, presented at the 11th International Display Workshops (IDW), Niigata, Japan, December 2004.
[12] W. Clemens, I. Fix, J. Ficker, A. Knobloch, A. Ullmann, *J. Mater. Res.* **2004**, *19*, 1963.
[13] C. D. Dimitrakopoulos, P. R. L. Malenfant, *Adv. Mater.* **2002**, *14*, 99.
[14] H. E. Katz, *Chem. Mater.* **2004**, *16*, 4748.
[15] G. Horowitz, *J. Mater. Res.* **2004**, *19*, 1946.

[16] H. Sirringhaus, P. J. Brown, R. H. Friend, M. M. Nielsen, K. Bechgaard, B. M. W. Langeveld-Voss, A. J. H. Spiering, R. A. J. Janssen, E. W. Meijer, P. Herwig, D. M. de Leeuw, *Nature* **1999**, *401*, 685.
[17] H. Sirringhaus, R. J. Wilson, R. H. Friend, M. Inbasekaran, W. Wu, E. P. Woo, M. Grell, D. D. C. Bradley, *Appl. Phys. Lett.* **2000**, *77*, 406.
[18] J. H. Burroughes, R. H. Friend, in *Conjugated Polymers* (Eds: J. L. Brédas, R. Silbey), Kluwer, Dordrecht, The Netherlands **1991**, pp. 555–622.
[19] J. Veres, S. D. Ogier, S. W. Leeming, D. C. Cupertino, S. M. Khaffaf, *Adv. Funct. Mater.* **2003**, *13*, 199.
[20] J. Veres, S. D. Ogier, G. Lloyd, D. de Leeuw, *Chem. Mater.* **2004**, *16*, 4543.
[21] L. L. Chua, P. K. H. Ho, H. Sirringhaus, R. H. Friend, *Appl. Phys. Lett.* **2004**, *84*, 3400.
[22] Z. Bao, A. Dodabalapur, A. J. Lovinger, *Appl. Phys. Lett.* **1996**, *69*, 4108.
[23] H. Sirringhaus, N. Tessler, R. H. Friend, *Science* **1998**, *280*, 1741.
[24] T. Bjornholm, T. Hassenkam, D. R. Greve, R. D. McCullough, M. Jayaraman, S. M. Savoy, C. E. Jones, J. T. McDevitt, *Adv. Mater.* **1999**, *11*, 1218.
[25] R. J. Kline, M. D. McGehee, E. N. Kadnikova, J. S. Liu, J. M. J. Frechet, *Adv. Mater.* **2003**, *15*, 1519.
[26] J. A. Merlo, C. D. Frisbie, *J. Phys. Chem. B* **2004**, *108*, 19 169.
[27] J. F. Chang, B. Q. Sun, D. W. Breiby, M. M. Nielsen, T. I. Solling, M. Giles, I. McCulloch, H. Sirringhaus, *Chem. Mater.* **2004**, *16*, 4772.
[28] N. Zhao, G. A. Botton, S. P. Zhu, A. Duft, B. S. Ong, Y. L. Wu, P. Liu, *Macromolecules* **2004**, *37*, 8307.
[29] G. M. Wang, J. Swensen, D. Moses, A. J. Heeger, *J. Appl. Phys.* **2003**, *93*, 6137.
[30] A. Zen, J. Pflaum, S. Hirschmann, W. Zhuang, F. Jaiser, U. Asawapirom, J. P. Rabe, U. Scherf, D. Neher, *Adv. Funct. Mater.* **2004**, *14*, 757.
[31] D. H. Kim, Y. D. Park, Y. S. Jang, H. C. Yang, Y. H. Kim, J. I. Han, D. G. Moon, S. J. Park, T. Y. Chang, C. W. Chang, M. K. Joo, C. Y. Ryu, K. W. Cho, *Adv. Funct. Mater.* **2005**, *15*, 77.
[32] H. Sirringhaus, N. Tessler, D. S. Thomas, P. J. Brown, R. H. Friend, in *Advances in Solid-State Physics*, Vol. 39 (Ed: B. Kramer), Vieweg, Wiesbaden, Germany, **1999**, pp. 101–110.
[33] M. S. A. Abdou, F. P. Orfino, Y. Son, S. Holdcroft, *J. Am. Chem. Soc.* **1997**, *119*, 4518.
[34] J. Ficker, A. Ullmann, W. Fix, H. Rost, W. Clemens, *J. Appl. Phys.* **2003**, *94*, 2638.
[35] J. Ficker, H. von Seggern, H. Rost, W. Fix, W. Clemens, I. McCulloch, *Appl. Phys. Lett.* **2004**, *85*, 1377.
[36] B. S. Ong, Y. L. Wu, P. Liu, S. Gardner, *J. Am. Chem. Soc.* **2004**, *126*, 3378.
[37] M. Heeney, C. Bailey, K. Genevicius, M. Shkunov, D. Sparrowe, S. Tierney, I. McCulloch, *J. Am. Chem. Soc.* **2005**, *127*, 1078.
[38] P. T. Herwig, K. Mullen, *Adv. Mater.* **1999**, *11*, 480.
[39] A. Afzali, C. D. Dimitrakopoulos, T. O. Graham, *Adv. Mater.* **2003**, *15*, 2066.
[40] G. H. Gelinck, T. C. T. Geuns, D. M. de Leeuw, *Appl. Phys. Lett.* **2000**, *77*, 1487.
[41] A. Afzali, C. D. Dimitrakopoulos, T. L. Breen, *J. Am. Chem. Soc.* **2002**, *124*, 8812.
[42] S. Aramaki, Y. Sakai, N. Ono, *Appl. Phys. Lett.* **2004**, *84*, 2085.
[43] P. C. Chang, J. Lee, D. Huang, V. Subramanian, A. R. Murphy, J. M. J. Frechet, *Chem. Mater.* **2004**, *16*, 4783.
[44] J. G. Laquindanum, H. E. Katz, A. J. Lovinger, *J. Am. Chem. Soc.* **1998**, *120*, 664.
[45] M. Mushrush, A. Facchetti, M. Lefenfeld, H. E. Katz, T. J. Marks, *J. Am. Chem. Soc.* **2003**, *125*, 9414.
[46] N. Stingelin-Stutzmann, E. Smits, H. Wondergem, C. Tanase, P. W. M. Blom, P. Smith, D. M. de Leeuw, *Nat. Mater.* **2005**, *4*, 601.
[47] A. M. van de Craats, N. Stutzmann, O. Bunk, M. M. Nielsen, M. Watson, K. Mullen, H. D. Chanzy, H. Sirringhaus, R. H. Friend, *Adv. Mater.* **2003**, *15*, 495.
[48] W. Pisula, A. Menon, M. Stepputat, I. Lieberwirth, U. Kolb, A. Tracz, H. Sirringhaus, T. Pakula, K. Müllen, *Adv. Mater.* **2005**, *17*, 684.
[49] I. McCulloch, W. M. Zhang, M. Heeney, C. Bailey, M. Giles, D. Graham, M. Shkunov, D. Sparrowe, S. Tierney, *J. Mater. Chem.* **2003**, *13*, 2436.
[50] L. L. Chua, J. Zaumseil, J. F. Chang, E. C. W. Ou, P. K. H. Ho, H. Sirringhaus, R. H. Friend, *Nature* **2005**, *434*, 194.
[51] H. E. Katz, A. J. Lovinger, J. Johnson, C. Kloc, T. Siegrist, W. Li, Y.-Y. Lin, A. Dodabalapur, *Nature* **2000**, *404*, 478.
[52] A. Babel, S. A. Jenekhe, *J. Am. Chem. Soc.* **2003**, *125*, 13 656.
[53] A. Facchetti, M. Mushrush, M. H. Yoon, G. R. Hutchison, M. A. Ratner, T. J. Marks, *J. Am. Chem. Soc.* **2004**, *126*, 13 859.
[54] C. Waldauf, P. Schilinsky, M. Perisutti, J. Hauch, C. J. Brabec, *Adv. Mater.* **2003**, *15*, 2084.
[55] E. J. Meijer, D. M. de Leeuw, S. Setayesh, E. Van Veenendaal, B. H. Huisman, P. W. M. Blom, J. C. Hummelen, U. Scherf, T. M. Klapwijk, *Nat. Mater.* **2003**, *2*, 678.
[56] A. Babel, J. D. Wind, S. A. Jenekhe, *Adv. Funct. Mater.* **2004**, *14*, 891.
[57] Y. Kunugi, K. Takimiya, N. Negishi, T. Otsubo, Y. Aso, *J. Mater. Chem.* **2004**, *14*, 2840.
[58] A. Facchetti, M.-H. Yoon, T. J. Marks, *Adv. Mater.* **2005**, *17*, 1705.
[59] C. J. Drury, C. M. J. Mutsaers, C. M. Hart, M. Matters, D. M. de Leeuw, *Appl. Phys. Lett.* **1998**, *73*, 108.
[60] H. Sirringhaus, T. Kawase, R. H. Friend, T. Shimoda, M. Inbasekaran, W. Wu, E. P. Woo, *Science* **2000**, *290*, 2123.
[61] R. A. L. Jones, R. W. Richards, *Polymers at Surfaces and Interfaces*, Cambridge University Press, Cambridge, UK **1999**.
[62] L. L. Chua, P. K. H. Ho, H. Sirringhaus, R. H. Friend, *Adv. Mater.* **2004**, *16*, 1609.
[63] L. A. Majewski, M. Grell, S. D. Ogier, J. Veres, *Org. Electron.* **2003**, *4*, 27.
[64] L. A. Majewski, R. Schroeder, M. Grell, *Adv. Mater.* **2005**, *17*, 192.
[65] M. Halik, H. Klauk, U. Zschieschang, G. Schmid, C. Dehm, M. Schutz, S. Maisch, F. Effenberger, M. Brunnbauer, F. Stellacci, *Nature* **2004**, *431*, 963.
[66] M.-H. Yoon, A. Facchetti, T. J. Marks, *Proc. Natl. Acad. Sci. USA* **2005**, *102*, 4679.
[67] H. G. O. Sandberg, T. G. Bäcklund, R. Österbacka, H. Stubb, *Adv. Mater.* **2004**, *16*, 1112.
[68] J. W. van der Horst, P. A. Bobbert, M. A. J. Michels, G. Brocks, P. J. Kelly, *Phys. Rev. Lett.* **1999**, *83*, 4413.
[69] J. L. Brédas, D. Beljonne, V. Coropceanu, J. Cornil, *Chem. Rev.* **2004**, *104*, 4971.
[70] P. J. Brown, H. Sirringhaus, M. G. Harrison, M. Shkunov, R. H. Friend, *Phys. Rev. B* **2001**, *63*, 125 204.
[71] Y. Deng, H. Sirringhaus, *Phys. Rev. B* **2005**, *72*, 045 207.
[72] D. Beljonne, J. Cornil, H. Sirringhaus, P. J. Brown, M. Shkunov, R. H. Friend, J. L. Brédas, *Adv. Funct. Mater.* **2001**, *11*, 229.
[73] R. Österbacka, C. P. An, X. M. Jiang, Z. V. Vardeny, *Science* **2000**, *287*, 839.
[74] R. A. Marcus, *Discuss. Faraday Soc.* **1960**, *29*, 21.
[75] H. Bässler, *Phys. Status Solidi B* **1993**, *175*, 15.
[76] S. V. Novikov, D. H. Dunlap, V. M. Kenkre, P. E. Parris, A. V. Vannikov, *Phys. Rev. Lett.* **1998**, *81*, 4472.
[77] M. C. J. M. Vissenberg, M. Matters, *Phys. Rev. B* **1998**, *57*, 12 964.
[78] C. Tanase, E. J. Meijer, P. W. M. Blom, D. M. de Leeuw, *Phys. Rev. Lett.* **2003**, *91*, 216 601.
[79] S. Shaked, S. Tal, Y. Roichman, A. Razin, S. Xiao, Y. Eichen, N. Tessler, *Adv. Mater.* **2003**, *15*, 913.
[80] A. Salleo, T. W. Chen, A. R. Volkel, Y. Wu, P. Liu, B. S. Ong, R. A. Street, *Phys. Rev. B* **2004**, *70*, 115 311.
[81] L. Buergi, H. Sirringhaus, R. H. Friend, *Appl. Phys. Lett.* **2002**, *80*, 2913.
[82] I. I. Fishchuk, A. Kadashchuk, H. Bässler, S. Nešpůrek, *Phys. Rev. B* **2003**, *67*, 224 303.

ADVANCED MATERIALS

[83] J.-F. Chang, H. Sirringhaus, unpublished.
[84] K. P. Puntambekar, P. V. Pesavento, C. D. Frisbie, *Appl. Phys. Lett.* **2003**, *83*, 5539.
[85] L. Buergi, T. J. Richards, R. H. Friend, H. Sirringhaus, *J. Appl. Phys.* **2003**, *94*, 6129.
[86] J. A. Nichols, D. J. Gundlach, T. N. Jackson, *Appl. Phys. Lett.* **2003**, *83*, 2366.
[87] B. H. Hamadani, D. Natelson, *Appl. Phys. Lett.* **2004**, *84*, 443.
[88] J. C. Scott, G. G. Malliaras, *Chem. Phys. Lett.* **1999**, *299*, 115.
[89] P. V. Pesavento, R. J. Chesterfield, C. R. Newman, C. D. Frisbie, *J. Appl. Phys.* **2004**, *96*, 7312.
[90] A. Facchetti, M. Mushrush, H. E. Katz, T. J. Marks, *Adv. Mater.* **2003**, *15*, 33.
[91] J. Kanicki, in *Thin Film Transistors* (Eds: C. R. Kagan, P. Andry), Marcel Dekker, New York **2003**, p. 71.
[92] M. Matters, D. M. de Leeuw, P. T. Herwig, A. R. Brown, *Synth. Met.* **1999**, *102*, 998.
[93] R. A. Street, A. Salleo, M. L. Chabinyc, *Phys. Rev. B* **2003**, *68*, 085 316.
[94] R. Schmechel, H. von Seggern, *Phys. Status Solidi A* **2004**, *201*, 1215.
[95] T. Lindner, G. Paasch, S. Scheinert, *J. Mater. Res.* **2004**, *19*, 2014.
[96] A. Salleo, R. A. Street, *Phys. Rev. B* **2004**, *70*, 235 324.
[97] A. Salleo, R. A. Street, *J. Appl. Phys.* **2003**, *94*, 4231.
[98] L. Buergi, T. Richards, M. Chiesa, R. H. Friend, H. Sirringhaus, *Synth. Met.* **2004**, *146*, 297.
[99] S. J. Zilker, C. Detcheverry, E. Cantatore, D. M. de Leeuw, *Appl. Phys. Lett.* **2001**, *79*, 1124.
[100] D. B. A. Rep, A. F. Morpurgo, W. G. Sloof, T. M. Klapwijk, *J. Appl. Phys.* **2003**, *93*, 2082.

